Raman Spectroscopic Studies on Single Supersaturated Droplets of Sodium and Magnesium Acetate

Liang-Yu Wang, Yun-Hong Zhang,* and Li-Jun Zhao

The Institute for Chemical Physics, School of Science, Beijing Institute of Technology, Beijing, China 100081

Received: September 13, 2004; In Final Form: November 9, 2004

Raman spectroscopy was used to study structural changes, in particular, the formation of contact-ion pairs in supersaturated aqueous $NaCH_3COO$ and $Mg(CH_3COO)_2$ droplets at ambient temperatures. The single droplets levitated in an electrodynamic balance (EDB), lost water, and became supersaturated when the relative humidity (RH) decreased. For $NaCH_3COO$ droplet the water-to-solute molar ratio (WSR) was 3.87 without solidification when water molecules were not enough to fill in the first hydration layer of Na^+, in favor of the formation of contact-ion pairs. However, the symmetric stretching vibration band (ν_3 mode) of free $-COO^-$ constantly appeared at 1416 cm^{-1}, and no spectroscopic information related to monodentate, bidentate, or bridge bidentate contact-ion pairs was observed due to the weak interactions between the Na^+ and acetate ion. On the other hand, the band of methyl deformation blue shifted from 1352 to 1370 cm^{-1} (at RH = 34.2%, WSR = 2.43), corresponding to the solidification process of a novel metastable phase in the highly supersaturated solutions. With further decreasing RH, a small amount of supersaturated solution still existed and was proposed to be hermetically covered by the metastable phase of the particle. In contrast, the interaction between Mg^{2+} and acetate ion is much stronger. When WSR decreased from 21.67 to 2.58 for the $Mg(CH_3COO)_2$ droplet, the band of C−C-symmetric stretching (ν_4 mode) had a blue shift from 936 to 947 cm^{-1}. The intensity of the two new shoulders (∼1456 and ∼1443 cm^{-1}) of the ν_3 band of free $-COO^-$ at 1420 cm^{-1} increased with the decrease of WSR. These changes were attributed to the formation of contact-ion pairs with bidentate structures. In particular, the small frequency difference between the shoulder at ∼1443 cm^{-1} and the ν_3 band of the free $-COO^-$ group (∼1420 cm^{-1}) was proposed to be related to the formation of a chain structure based on the contact-ion pairs of bridge bidentate. The continuous formation of various contact-ion pairs started at higher WSR value (WSR = 15.5) greatly reduced the hygroscopic properties of $Mg(CH_3COO)_2$ droplet, so that the WSR of $Mg(CH_3COO)_2$ droplets was even lower than that of $NaCH_3COO$ in the RH range of 40−60%.

1. Introduction

Due to their important hygroscopic properties, atmospheric aerosols have greatly intrigued both aerologists and chemists. The change of the solution concentrations of aqueous aerosol particles through altering the relative humidity (RH) will affect the physical and chemical properties of aerosols, e.g., the size distributions, radiative properties, deposition characteristics, and chemical reactivity. Many experiments have already been carried out to understand the hygroscopic nature of the aerosols.[1−7] Gravimetric analysis was used to measure the hygroscopicity of filter samples.[1] The EDB (electrodynamic balance) has been used to operate the relative mass measurements by levitating the single particles.[2−4] FTIR spectroscopy combined with an aerosol flow tube was utilized to study the hygroscopic properties according to the changes of water peak area.[5−7]

The sodium and magnesium ions are the major cations in the sea-salt aerosols, and their salts of the same anions have very different hygroscopic properties.[8,9] From a molecular level, this difference is controlled by the interactions between water molecules and solutes, including the hydration of ions, formation of ion pairs, as well as hydrogen bonding between water molecules. In our previous work Raman spectroscopy coupled with EDB was used to investigate the relationship between the solute−water interactions and the hygroscopicity for their sulfate and nitrate salts, including $MgSO_4$,[10] $Na_2SO_4/MgSO_4$ mixture,[11] and $Mg(NO_3)_2$.[12] From those studies it was found that there is a good relationship between the transition of the hygroscopicity and the formation of contact-ion pairs. In addition, the structure of water molecules in $NaClO_4$ and $Mg(ClO_4)_2$ solutions was studied from diluted concentrations to high supersaturations,[13] revealing the existence of water monomers in highly supersaturated droplets.

Besides the inorganic salts, the atmospheric aerosols often consist of organic salts. Many recent studies found that the organic compounds could contribute as much as 25−50% of total carbon in aerosols.[14] The organic aerosols could change the hygroscopic properties of the inorganic fraction both positively and negatively.[15−19] At the same time, the organic salts played an important role in the formation of cloud condensation nuclei and visibility degradation.[20,21] However, there are very limited studies on supersaturated solutions of organic salts at a molecular level.

The acetate has advantages of low molecular weight, atmospheric importance, and low volatility for ease of water activity measurements. Compared with sulfate or nitrate ion, acetate ion, composed of a carboxyl group and a single methyl group, has a large dipole moment (∼5D). The interactions between acetate anion and its surrounding metal ions are expected to be significant, and hence, the ion pairs are easy to form, especially

* To whom correspondence should be addressed. Phone: 86-10-86668406. Fax: 86-10-68912652. E-mail: yhz@bit.edu.cn.

10.1021/jp0458811 CCC: $30.25
Published on Web 01/06/2005

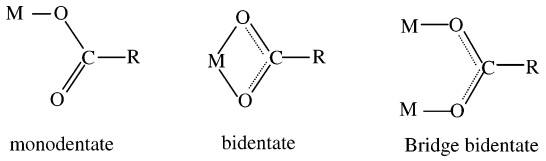

Figure 1. Structures of contact-ion pairs of metal and acetate ion.

for Mg^{2+} having a large charge-to-radius ratio. Even though a single droplet containing Mg^{2+} is generally observed to be more hygroscopic than that carrying Na^+ with the same inorganic anions,[12,13] the water content of $Mg(CH_3COO)_2$ droplet may be lower than that of $NaCH_3COO$ due to reduction of the hygroscopicity once Mg^{2+} forms contact-ion pairs with CH_3COO^-. In addition, the interaction of acetate ions with metal atoms is of further interest because it is also among humic substances.[22,23] Therefore, the acetate ion was studied here not only because it appears in the environment either as a metabolic product of microorgnaisms[24] or through decomposition of humic acids in some industrial conditions,[25] but also as a reference to organic complexation.

In general, there are three representative typical structures of contact-ion pairs for the acetate group combined with metal ions: unidentate (or monodentate), bidentate, and bridge bidentate (shown in Figure 1).[26,27] The metal ion in the bidentate form interacts equally with two oxygen atoms of the CH_3COO^- group, but in monodentate form, it interacts only with one of those oxygen atoms. In the bridge bidentate form two metal ions each interact with one of the two oxygen atoms of the same acetate group. Vibration spectroscopy, i.e., both IR and Raman, could approach these structural problems from the molecular level. In particular, Raman spectroscopy was used even more extensively because the Raman spectra of aqueous acetate solutions were easy to obtain and could bring additional data.[28−32] Previous studies[33] involving ion pairing of alkalis with complex ligands in relatively dilute solutions showed that there were no dramatic effects on the frequencies, peak positions, and the half-widths of the internal modes of the ligands. In contrast, the association of alkaline earths with complex ligands could affect the internal modes of the ligands.[25,34] This is probably because alkaline earths have a larger charge-to-radius ratio than the alkalis in the same period, which is in more favor of the formation of contact-ion pairs than that of the solvent-separated ion pairs in aqueous solutions. However, most of the above experiments were limited to dilute concentrations because of the saturation constraints in bulk samples.

Under highly supersaturated conditions the interactions between the cations and acetate can be predicted to be stronger, which facilitates the formation of various contact-ion pairs, so that some new and novel properties may arise. In the present study the hygroscopic properties of sodium and magnesium acetate droplets were investigated with the combination of Raman spectroscopy and EDB. The formation of contact-ion pairs and their effects on the hygroscopic properties of the solutions were discussed in sodium magnesium acetate solutions up to extremely high concentrations.

2. Experimental Methods

Consisting of a single droplet in an electric field in the EDB enables measuring the hygroscopic properties of aerosols of inorganic salts, organic salts, and organic acids, which have been extensively examined. One of the advantages of the EDB technique is that a droplet can be levitated under precise control. Thus, heterogeneous nucleation is suppressed and the droplets

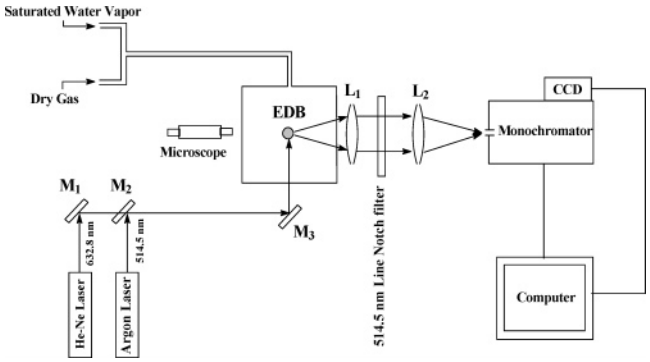

Figure 2. Schematic diagram of the EDB−Raman system.

usually achieve the supersaturated state before crystallization. The EDB device consists of a pair of DC end cap electrodes and an AC ring electrode. A piezoelectric particle generator (Uni-Photon-Inc., model 201) was used to eject the droplets of a dilute solution, which were charged by induction before entering the EDB. The high-voltage AC electrode was used to trap a single charged droplet oscillating around the center of the balance. The electrostatic force imposed on the droplet by the DC voltage was adjusted to balance the changing weight of the droplet with RH and keep the droplet stationary at the center of the EDB. The applied balancing DC voltage was proportional to the mass of the levitated particle. When a droplet was equilibrated with the surrounding environment in the EDB, the water activity (a_w) of the droplet was related to the RH by $a_w = P_w/P_w^{sat} = RH/100$. P_w and P_w^{sat} correspond to the partial pressure of water of air flow and the saturation water vapor pressure at the ambient temperatures, respectively. By reference to the DC voltage value for some state with known composition at certain RH (their saturated bulk solutions), the water to solute molar ratio (WSR) of the droplet was known through DC balancing voltage measurements and could be changed by altering the ambient RH. In this study the experimental setup and procedures were similar to our previous works.[6,7,10,11] Figure 2 shows the schematic diagram of the apparatus for the water cycle and Raman scattering measurements of levitated droplets. Illuminated by a He−Ne laser, a microscope at 20× magnification was used to observe a charged droplet held stationary at the center of the EDB. To adjust the RH, a stream of saturated air and another of dry air were mixed at controlled flow rates. The flow air for control of RH in the EDB was momentarily stopped when the balancing voltage was measured. The RH was determined by a dew-point hygrometer (EG&G DEW Prime model 2000). The size of the droplets studied was about 30−60 μm. The water activities of the bulk solutions were measured by an AquaLab water activity meter (model series III, Decagon Device, Inc).

A Raman system, consisting of a 5 W argon-ion laser (Coherent 190−5) and a 0.5 m monochromator (Acton SpectraPro500) attached to a CCD detector (Princeton Instrument, TE/CCD-1100PFUV), was incorporated into the EDB system. The output power of the 514.5 nm excitation line was between 800 and 1000 mW. A pair of lenses, which matches the *f*/6.9 optics of the monochromator, was used to focus the 90° scattering of the levitated droplet on the slit of the monochromator. A 514.5 nm Raman notch filter was placed between the two lenses to remove the strong Rayleigh scattering. The 1200 g/mm grating of the monochromator was selected to obtain the Raman spectra of the droplet with a high spectral resolution of about 2.3 cm^{-1}. All measurements were made at ambient temperatures

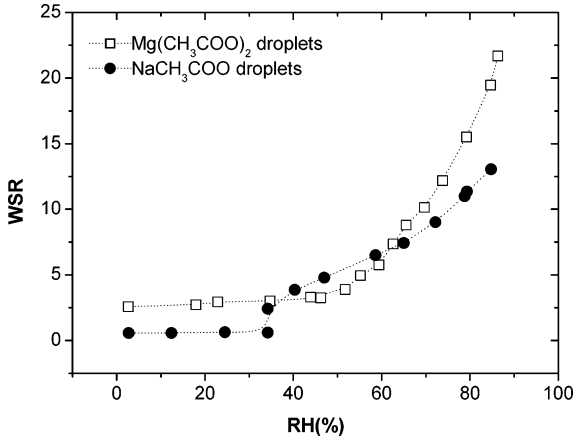

Figure 3. Water-to-solute molar ratio (WSR) of sodium acetate droplets and magnesium acetate droplets at various RH.

of 22−24 °C. The spectra reported in this work were the averages of the 30 frames, each with an accumulation time of about 5 s.

3. Results and Discussions

3.1. Hygroscopic Properties of Sodium and Magnesium Acetate Droplets. To relate the Raman spectra to the WSR of the supersaturated droplets, the compositional dependence of the droplet on RH was determined. Figure 3 shows the hygroscopic properties of $NaCH_3COO$ (closed circles) and $Mg(CH_3COO)_2$ (open squares) droplets in terms of equilibrium WSR as a function of RH. These measurements were made when RH was decreased in steps. Solidification, leading to a sudden decrease in WSR, began to appear when the RH arrived at 34.2% for $NaCH_3COO$ droplets, which was much lower than the reference state, i.e., the saturation point of $NaCH_3COO\cdot 3H_2O$ bulk solution (RH = 76%, WSR = 9.45), and then at the same RH, solidification would continue as long as WSR was 0.6. By decreasing RH further, the small amount of water (WSR $\approx$ 0.5) still remained.

For magnesium acetate droplets, the bulk saturated solution of $Mg(CH_3COO)_2\cdot 4H_2O$ (RH = 65%, WSR = 8.8) was chosen as the reference state. The WSR of $Mg(CH_3COO)_2$ droplets decreased continuously from 21.7 to 3.3 when RH decreased from 86.3% to 43.9%. As the RH further decreased from 43.9% to 2.6%, the ratio decreased only slightly. Different from sodium acetate droplets, the magnesium acetate droplets did not crystallize even at the lowest WSR of 2.58 in this experiment. Such low WSR, at which there were not enough water molecules to fulfill the first shell of the hydration layer of Mg^{2+}, could facilitate the formation of various kinds of contact-ion pairs, similar to the previous observations on the $MgSO_4$[10] and $Mg(NO_3)_2$[12] droplets. The most interesting fact is that the WSR values of Mg $(CH_3COO)_2$ were found to be smaller than that of $NaCH_3COO$ in the RH range from 60% to 40%, which was different from previous observations on the salts of magnesium and sodium[12,13] and will be discussed below.

Since the C−O-symmetric stretching (ν_3 mode), the C−C-symmetric stretching (ν_4 mode), and the methyl deformation (ν_9 mode) were found to be sensitive to the formation of contact-ion pairs, insight into the supersaturated droplets should be obtained through analysis of these bands.

3.2. Raman Spectra and Formation of Contact-Ion Pairs. The vibration spectra of the acetate ions in sodium acetate have been assigned in terms of a C_{2v} molecular symmetry, assuming free rotation of the CH_3 group around the C−C bond.[35,36] The 15 fundamental modes of acetate ions are classed in $5A_1(\nu_1,\nu_2,\nu_3,\nu_4,\nu_5)$, $1A_2(\nu_6)$, $5B_1(\nu_7,\nu_8,\nu_9,\nu_{10},\nu_{11})$, and $4B_2(\nu_{12},\nu_{13},\nu_{14},\nu_{15})$ modes, in which the $5A_1$, 5B1, and $4B_2$ modes are all infrared and Raman active while only the A_2 mode, methyl torsion, is Raman active but infrared inactive.

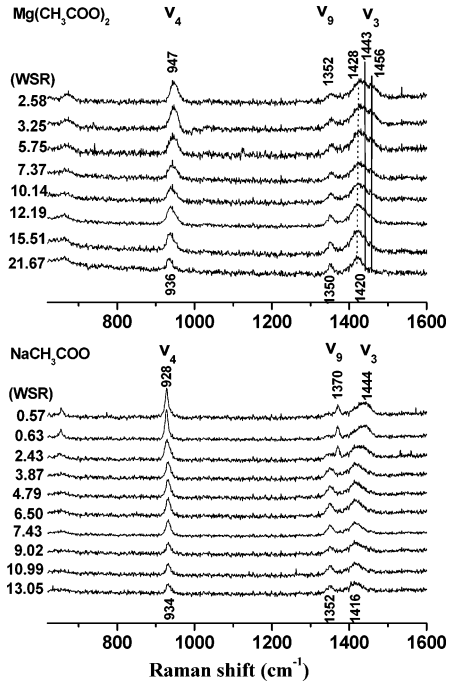

Figure 4. Raman spectra of $Mg(CH_3COO)_2$ and $NaCH_3COO$ droplets at various molar water-to-solute ratios (WSR).

The Raman spectra of the droplets of magnesium and sodium acetate solutions at various WSR in the region of 600−1600 cm^{-1} are shown in Figure 4. The three main kinds of vibration modes, namely, the ν_3, ν_4, and ν_9 modes, have been labeled in the Figures. For the $NaCH_3COO$ droplets, when WSR deceased from 13.05 to 3.87, the band of the ν_3 mode constantly appeared at 1416 cm^{-1}. No obvious changes were observed for the ν_4 and ν_9 bands. However, a sudden spectral change happened in the beginning of the solidification process when WSR was 2.43. A new sharp strong band, corresponding to the solid phase, appeared at 1370 cm^{-1} accompanying the decrease of the band at 1352 cm^{-1} of the supersaturated solutions. At the same time the ν_4 band, which had a red shift from 934 to 928 cm^{-1}, also became sharper and stronger. The ν_3 band was getting broad moving from 1416 to 1444 cm^{-1}. For the droplets of $Mg(CH_3COO)_2$ the peak maximum of the ν_3 mode appeared at 1420 cm^{-1} at the diluted state (WSR = 21.67), corresponding to the free acetate ion as the main component. When WSR arrived at 2.58, the peak maximum shifted to 1428 cm^{-1}, and two shoulders at 1443 and 1456 cm^{-1} increased with the decrease of WSR. At the same time the band of the ν_4 mode had a blue shift from 936 to 947 cm^{-1}. The ν_9 band at 1350 cm^{-1} had no obvious changes with the decrease of WSR except that its intensity became weaker than before.

Table 1 gives a detailed description of the Raman bands and their vibrational assignments for three states of sodium and magnesium acetate. There has been a lot of spectroscopy research on the interaction between the $-COO^-$ group and metal ions[35,37−40] as well as water molecules.[36] The ν_3 mode was strong and polarized in the Raman spectra and the most sensitive band to the microenvironments of the $-COO^-$ group, even though it was very close to the $-CH_3$ deformation modes (ν_9 and ν_{13}) in the region of 1400−1500 cm^{-1}. In solid sodium

TABLE 1: Raman Wavenumbers and Vibrational Assignments for Sodium and Magnesium Acetate[a]

	$NaCH_3COO$			$Mg(CH_3COO)_2$		
vibrational assignment	dilute/ supersaturated	trihydrated solid[29]	metastable solid (this work)	dilute	tetrahydrated solid[29]	supersaturated (this work)
ν_3 C−O str	1416	1414	1419	1420	1421	1428 1443 1456
ν_4 C−C str	934	924	928	936	947	947
ν_9 CH_3 def	1352	1350	1370	1350	1350	1352

[a] str, stretching; def, deformation.

acetate trihydrate and solid magnesium acetate tetrahydrate the ν_3 band appeared at 1414 and 1421 cm^{-1}, respectively.[29] By using the ab initio molecular orbital method Masayuki et al.[41] concluded that the interaction between $-COO^-$ and Mg^{2+} was stronger than that between COO^- and Na^+, which also applied to sodium and magnesium acetate solutions. It was found that the solution and solid-state spectra of $NaCH_3COO{\cdot}3H_2O$ were identical.[42] However, in the present study the spectroscopic characteristic of the solid phase was different from that of the thermodynamically stable $NaCH_3COO{\cdot}3H_2O$ (seeing Table 1). In addition, the supersaturated solutions coexisted with the metastable solid phase in a wide RH range from 34.2% to 2.7% according to the continuous decrease of the intensity of the ν_4 band of the supersaturated solutions (at ~1352 cm^{-1}). The small amount of water, observed in NaCl aerosol particles, was considered to be either physically trapped within the aerosol particle or very strongly chemically bound to the NaCl.[43] The efflorescence products of the single levitated $H_2SO_4/NH_3/H_2O$ aerosol particles were also proposed as a structure of the polycrystalline material with several open but liquid-filled cavities or solid polycrystalline shell with embedded liquid.[44] In light of the above result, the supersaturated solutions were proposed to be trapped within the metastable solid phase. Due to the weak interactions between the Na^+ and acetate ion, no spectroscopic information related to monodentate, bidentate, or bridge bidentate contact-ion pairs was observed in the supersaturated solutions. The phase transition was the main cause of bands' development in the solidification process. A structural characteristic of the metastable solid phase is that the $-CH_3$ group lost its rotational freedom around the C−C bond according to the appearance of the sharp band at 1370 cm^{-1}.

In contrast, in magnesium acetate solutions there were three different components of the symmetric C−O stretching, corresponding to the ν_3 vibration of the free acetate ion and the mono- and bidentate complexes.[45] Referring to the above discussion, there were two shoulders at 1443 and 1456 cm^{-1}, respectively. The C−O-symmetric stretching for the contact-ion pairs of the bidentate formed by copper and acetate was found to appear at ~1448 cm^{-1} by Quiles et al.,[42] and by using ab initio calculations Masayuki et al.[41] predicted that the ν_3 band in the bidentate form of magnesium should appear at ~1460 cm^{-1}. For some molecular systems it was possible to directly compare the experimental vibrational frequencies to those predicted from ab initio calculations or density functional theory in order to learn more about the structure, properties, and environment of the molecules. For example, hydrogen-bonding effects on vibrational spectra were studied this way for several systems and useful in elucidating why some bands blue shift or red shift noticeably.[46−48] For the systems investigated here, these types of comparisons would also be useful and provide even more insight into the intriguing and sensitive vibrational frequency shifts observed in the experiments. Therefore, the band at 1456 cm^{-1} in our observation must be attributed to the contact-ion pairs of bidentate complexes by Mg^{2+} and acetate. For the 1443 cm^{-1} band it was hard to know which kind of complexes to attribute it to because it has not been reported before. Chan et al.[49] found that mass-transfer limitation exists in the supersaturated state for both $MgSO_4$ and $Mg(CH_3COO)_2$ droplets. They suggested that gel phases instead of crystallization were formed at the low RH. In addition, "polymeric" contact-ion pair chains were proposed for the gel state of $MgSO_4$ aerosol at low RH by Zhang et al.[10] Hence, we could expect the complexes of the band at 1443 cm^{-1} should be similar to the contact-ion pair chains of $MgSO_4$. Here, we proposed a chain structure connected by the bridge bidentate of $Mg(CH_3COO)_2$ for the expression of the gel state, which is shown in Figure 5. Theoretically, according to the correlation between $\Delta\nu_{a-s}$ (frequency separation between the COO^- antisymmetric and symmetric stretching) and the types of COO^- coordination investigated in previous studies,[26,41] the structure of contact-ion pairs could also be possibly predicted. Deacon and Phillips[26] founded an empirical rule to correlate $\Delta\nu_{a-s}$ with the types of coordination of the COO^- group with divalent metal cations, which was in the form of $\Delta\nu_{a-s}$ (monodentate) > $\Delta\nu_{a-s}$ (ionic) ≈ $\Delta\nu_{a-s}$ (bridging) > $\Delta\nu_{a-s}$ (bidentate). The rule showed that the frequency of symmetric stretching should shift to the higher wavenumber while that of antisymmetric stretching should shift to the lower wavenumber on formation of bidentate complexes. On the basis of these results, the band at ~1443 cm^{-1} in our observation, which shifted less (about 23 cm^{-1}) to the higher wavenumber relative to the free ν_3 band (at 1420 cm^{-1}) than the bidentate form (about 36 cm^{-1}), should correspond to the bridging chain structure as Figure 5 shows. Masayuki et al.[41] calculated the structure parameters of different complexes of magnesium acetate. For the free acetate ion, the lengths of two C−O bonds were 1.24 Å and the angle of O−C−O was 127.5°, indicating that the $-COO^-$ group was symmetric. For the monodentate complex the C−O bond interacting with Mg^{2+} was 1.30 Å longer than the other C−O bond with a length of 1.21 Å, while there was a little change for the O−C−O angle (125.3°). The $-COO^-$ group of the acetate ion in the bidentate form was nearly symmetric, and the lengths of two C−O bonds were, 1.26 Å, similar to the free acetate ion, but the O−C−O angle was 117.8°, much smaller than that of the free acetate ion. Considering the similarity between the bidentate contact-ion pairs and the bridging chain structure, we expected that the structural rearrangement would mainly come from the change

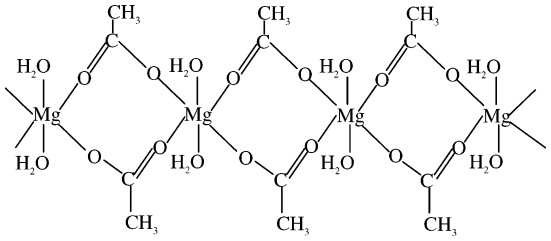

Figure 5. Chain structure of the bridging bidentate of $Mg(CH_3COO)_2$.

of the O−C−O angle rather than the C−O bond when the chain structure formed.

The fwhh (full-width at half-height) of the ν_9 band was almost constant in the formation process of various contact-ion pairs, indicating that the $-CH_3$ group retains rotation freedom around the C−C bond in the contact-ion pairs, different from the metastable solid phase of the $NaCH_3COO$ particle.

Different from most of the observations on salts of magnesium and sodium,[12,13] the droplet of $Mg(CH_3COO)_2$ has less water than that of $NaCH_3COO$ when RH decreased from 60% to 40%, as mentioned above. In general, Mg^{2+} has a strong tendency to retain its hexahydrated structure because of its high hydration energy, leading to the stable hydrated ions of $Mg(H_2O)_6^{2+}$. Thus, the contact-ion pairs formed only at WSR below 6, i.e., the anions could penetrate the first solvation shell only when there were not sufficient water molecules to retain the hexahydrated structure of Mg^{2+}.[12,13] In this work formation of the bidentate contact-ion pairs between Mg^{2+} and CH_3COO^- was found starting at WSR = 15.5, indicating that the interactions between Mg^{2+} and CH_3COO^- in the bidentate $[Mg(H_2O)_4OOCCH_3]$ should be stronger than that between Mg^{2+} and H_2O in $[Mg(H_2O)_6]$. The continuous formation of various contact-ion pairs would greatly reduce the hygroscopicity of Mg^{2+}, which was the reason that the WSR of the $Mg(CH_3COO)_2$ droplet was lower than that of $NaCH_3COO$ in the RH range of 40−60%.

The Raman spectra in the ν_4 mode region also provided useful information concerning the existence of complexes. Due to its high scattering activity and sensitive response to the environment of carboxyl group of the acetate, the C−C band is best suited to provide quantitative information. Moreover, it is located far away from other vibrations and consequently was less influenced by the overlapping bands.[25] The ν_4 band was observed at 930 cm^{-1} in aqueous solutions of sodium acetate,[28] and it shifted to higher wavenumbers upon complexation with a metal cation like Mg^{2+} or Ni^{2+} but did not with alkali metal cations such as K^+ or Na^+. The changes with WSR of peak position and fwhh of the C−C stretching band of $NaCH_3COO$ and Mg $(CH_3COO)_2$ are shown in Figure 6, from which it can be seen that the most distinct difference between the spectra of the two species was the changes of the peak position and fwhh of the C−C band at highly supersaturated concentrations. The strongest band of the $NaCH_3COO$ droplets had an overall red shift from 934 to 928 cm^{-1} and a decrease of its fwhh from 13.5 to 9.5 cm^{-1} when WSR decreased from 13.05 to 0.57. The spectral changes with WSR could be roughly divided into two sections. For the WSR between 13.5 and 2.43, the spectral response was not sensitive to the ratio even though the solutions already became supersaturated with WSR smaller than 8.0. However, the spectral response was a very sensitive function of WSR between 2.43 and 0.57 when the peak position and fwhh abruptly changes corresponding to the solidification process. These values are in good agreement with previously published data[25,28,50] in which the C−C vibration of the free acetate ion has been determined in the range 926−930 cm^{-1}. The fact proved once again the weak and negligible disturbance on acetate anions from the formation of contact-ion pairs in supersaturated droplets of sodium acetate. On the other hand, in $Mg(CH_3COO)_2$ droplets the peak position had a blue shift from 936 to 947 cm^{-1} and its fwhh increased from 16.7 to 27.8 cm^{-1} when WSR changed from 21.67 to 2.58. This spectral change has been attributed to transformation of free acetate ions to the contact-ion pairs of Mg^{2+} and CH_3COO^-.[51] Using the least-squares curve-fitting method the C−C band has been resolved into three components: the band of free acetate ion at 930 cm^{-1}, the band of monodentate complexes at 939 cm^{-1}, and the band of bidentate complexes at 947 cm^{-1}.[44] This indicated that the monodentate and bidentate complexes had C−C vibrations in the Raman spectra with different but close wavenumbers.

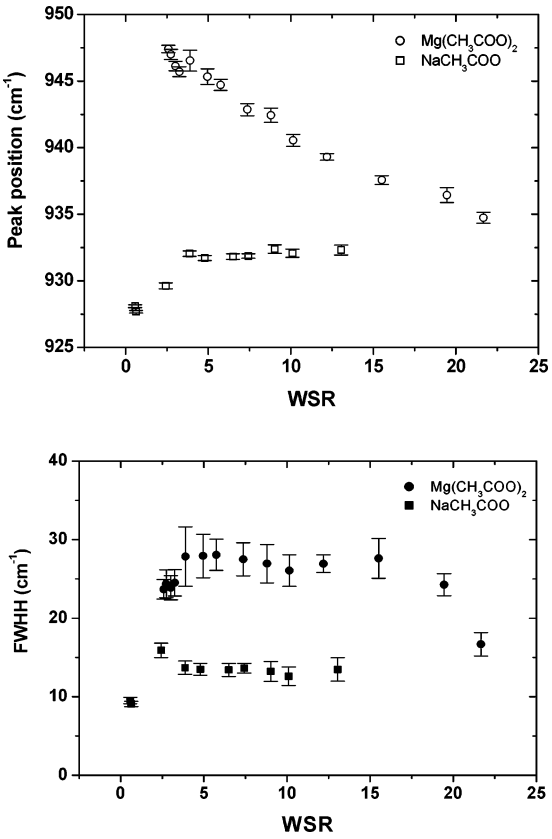

Figure 6. Dependence of the peak position and fwhh of the C−C-symmetric stretching band on the water-to-solute ratios.

4. Conclusions

Combining the single-particle levitation technique and in-situ Raman spectroscopy, the Raman spectra of organic salts droplets, i.e., single $NaCH_3COO$ and Mg $(CH_3COO)_2$ droplets in highly supersaturated states, has been obtained. For $NaCH_3COO$ droplets, when the WSR decreased to 2.43, the band of methyl deformation had a blue shift from 1352 to 1370 cm^{-1}, which showed the occurrence of a phase transition. The supersaturated solutions were proposed to be trapped within the metastable solid phase. However, no obvious formation of contact-ion pairs has ever been found due to the weak interactions between Na^+ and acetate ion. In contrast, the interactions between Mg^{2+} and acetate ion were stronger, which facilitated formation of contact-ion pairs. The shoulder at ∼1456 cm^{-1} has been considered as an indicator for formation of bidentate complexes of $Mg(CH_3COO)_2$ droplets in highly saturated solutions. The band at ∼1443 cm^{-1} was believed to have a chain structure composed of the contact-ion pair of bridge bidentate in highly supersaturated $Mg(CH_3COO)_2$ solutions. The formation of the bidentate contact-ion pairs between Mg^{2+} and CH_3COO^- was found to start at WSR = 15.5. The formation of contact-ion pairs greatly reduced the hygroscopicity of magnesium acetate aerosol, so that the WSR was found to be lower than that of $NaCH_3COO$ in the RH range of 40−60%. Hence, the EDB/Raman system is a unique and useful tool to probe the interactions between ions in supersaturated solutions of organic systems on a molecular level.

Acknowledgment. The experiments were conducted in the Department of Chemical Engineering at the Hong Kong University of Science and Technology. The financial support of the HKUST Postdoctoral Research Fund, the NSFC (20073004, 20473012), and the Trans-Century Training Program Foundation for the Talents by the Ministry of Education of China are gratefully acknowledged.

References and Notes

(1) Wrinkler, P. *Phys. Scr*. **1988**, *37*, 223.
(2) Tang, I. N.; Munkelwitz, H. R. *J. Geophys. Res.* **1994**, *99* (D9), 18801.
(3) Cohen, M. D.; Flagan, R. C.; Seinfeld, J. H. *J. Phys. Chem*. **1987**, *91*, 4563.
(4) Chan, C. K.; Flagan, R. C.; Seinfeld, J. H. *Atmos. Environ*. **1992**, *26A* (9), 1661.
(5) Onasch, T. B.; Siefert, R. L.; Brooks, S. D. *J. Geophys. Res.* **1999**, *104*, 21317.
(6) Han, F. H.; Martin, S. T. *J. Geophys. Res.* **1999**, *104* (D3), 3543.
(7) Cziczo, D. J.; Abbatt, J. P. D. *J. Geophys. Res.* **1999**, *104*, 13781.
(8) Ha, Z.; Chan, C. K. *Aerosol Sci. Technol.* **1999**, *31*, 154.
(9) Chan, C. K.; Ha, Z.; Choi, M. Y. *Atmos. Environ.* **2000**, *34*, 4795.
(10) Zhang, Y. H.; Chan, C. K. *J. Phys. Chem. A* **2000**, *104*, 9191.
(11) Zhang, Y. H.; Chan, C. K. *J. Phys. Chem. A* **2002**, *106*, 285.
(12) Zhang, Y. H.; Choi, M. Y.; Chan. C. K. *J. Phys. Chem. A* **2004**, *108*, 1712.
(13) Zhang, Y. H.; Chan, C. K. *J. Phys. Chem. A* **2003**, *107*, 5956.
(14) Sempéré, R.; Kawamura, K. *Atmos. Environ.* **1994**, *28* (3), 449.
(15) Choi, M. Y.; Chan, C. K. *Environ. Sci. Technol.* **2002**, *36*, 2422.
(16) Peng, C. G.; Chan, C. K. *Atmos. Environ.* **2001**, *35*, 1183.
(17) Choi, M. Y.; Chan, C. K. *J. Phys. Chem. A* **2002**, *106*, 4566.
(18) Peng, C. G.; Chan, M. N.; Chan, C. K. *Environ. Sci. Technol.* **2001**, *35*, 4495.
(19) Na, H. S.; Arnold, S.; Myerson, A. S. *J. Cryst. Growth* **1995**, *149*, 229.
(20) Eichel, C.; Kramer, M.; Wurzler, S. *J. Geophys. Res.* **1996**, *101* (D23), 29499.
(21) Cruz, C. N.; Pandis, S. N. *J. Geophys. Res.* **1998**, *103* (D11), 13111.
(22) Kinniburgh, D. G.; Milne, C. J.; Benedetti, M. F. *Environ. Sci. Technol.* **1996**, *30*, 1687.
(23) Filella, M.; Parthasarathy, N.; Buffle, J. *Humic and fulvic compounds, Encyclopedia of Analytical Science*; Academic Press: London, 1995; p 2017.
(24) Berthelin, *J. Pedologie, Gand.* **1982**, *32*, 313.
(25) Semmler, J.; Irish, D. E.; Oseki, T. *Geochim. Cosmochim. Acta*. **1990**, *54*, 947.
(26) Deacon, G. B.; Phillips, R. *J. Coord. Chem. Rev.* **1980**, *33*, 227.
(27) Yang, M. M.; Crerar, D. A.; Irish, D. E. *Geochim. Cosmochim. Acta* **1989**, *53*, 319.
(28) Bickley, R. I.; Edwards, H. G. M.; Rose, S. J.; Gustar, R. *J. Mol. Struct.* **1990**, *238*, 15.
(29) Frost, R. L.; Kloprogge, J. T. *J. Mol. Struct.* **2000**, *526*, 131.
(30) Frantz, J. D. *Chem. Geol.* **2000**, *164*, 1.
(31) Frost, R. L.; Kristof, J.; Schmidt, J. M.; Kloprogge, J. T. *Spectrochim. Acta, A* **2001**, *57*, 603.
(32) Koleva, V.; Stoilova, D. *J. Mol. Struct.* **2002**, *611*, 1.
(33) Spohn, P. D.; Brill, T. B. *J. Phys. Chem.* **1989**, *93*, 6224.
(34) Frantz, J. D.; Dubessy, J.; Mysen, B. O. *Chem. Geol.* **1994**, *116*, 181.
(35) Heyns, A. M. *J. Mol. Struct.* **1972**, *11*, 93.
(36) Marcus, Y. *Recl. Chem. Prog*. **1966**, *27*, 105.
(37) Baraldi, P.; Fabbri, G. *Spectrochim. Acta* **1981**, *37A*, 89.
(38) Johnson, M. K.; Powell, D. B.; Cannon, R. D. *Spectrochim. Acta* **1981**, *37A*, 899.
(39) Raghuvanshi, G. S.; Pal, M.; Patel, M. B.; Bist, H. D. *J. Mol. Struct*. **1983**, *101*, 7.
(40) Raghuvanshi, G. S.; Khandelwal, D. P.; Bist, H. D. *Appl. Spectrosc*. **1984**, *38*, 710.
(41) Masayuki, N.; Hajime, T.; Missuo, T. *J. Phys. Chem*. **1996**, *100*, 19812.
(42) Quiles, F.; Burneau, A. *Vib. Spectrosc*. **1998**, *16*, 105.
(43) Cziczo, D. J.; Nowak, J. B.; Hu, J. H.; Abbatt, P. D. *J. Geophys. Res.* **1997**, *102*, 18843.
(44) Colberg, C. A.; Krieger, U. K.; Peter, T. *J. Phys. Chem. A* **2004**, *108*, 2700.
(45) Nickolov, Zh.; Ivanov, I.; Georgive, G.; Stoilova, D. *J. Mol. Struct.* **1996**, *377*, 13.
(46) Geppert, W. D.; Ullrich, S.; Dessent, C. E. H.; Klaus, M. D. *J. Phys. Chem. A* **2000**, *104*, 11870.
(47) Rostkowska, H.; Nowak, M. J.; Lapinski, L.; Adamowicz, L. *Phys. Chem. Chem. Phys.* **2001**, *3*, 3012.
(48) Raveendran, P.; Zimmermann, D.; Häber, T.; Suhm, M. A. *Phys. Chem. Chem. Phys.* **2000**, *2*, 3555.
(49) Chan, C. K.; Flagan, R. C.; Seinfeld, J. H. *J. Am. Ceram. Soc.* **1998**, *81* (3), 646.
(50) Ito, K.; Bernstein, H. J. *Can. J. Chem.* **1956**, *34*, 170.
(51) Raghuvanshi, G. S.; Khandelwal, D. P.; Bist, H. D. *Spectrochim. Acta* **1985**, *41*, 391.